

COMPARISON OF MAGNETIC-GEARED PERMANENT-MAGNET MACHINES

X. Li¹, K.-T. Chau², M. Cheng^{1, *}, and W. Hua¹

¹School of Electrical Engineering, Southeast University, Nanjing 210096, China

²Department of Electrical and Electronic Engineering, The University of Hong Kong, Hong Kong, China

Abstract—With the advent of magnetic gears, researchers have developed a new breed of permanent-magnet machines. These magnetic-gear permanent-magnet machines artfully incorporate the concept of magnetic gearing into the permanent-magnet machines, leading to achieve low-speed high-torque direct-drive operation. In this paper, a quantitative comparison of three viable magnetic-gear permanent-magnet machines is firstly performed, hence revealing their key features, merits, demerits and applications. Initially, the development of the magnetic gears, including the converted topologies and field-modulated topologies, is reviewed. Then, three viable magnetic-gear permanent-magnet machines are identified and discussed. Consequently, the corresponding performances are analyzed and quantitatively compared. The results and discussions form an important foundation for research in low-speed high-torque direct-drive systems.

1. INTRODUCTION

Gears and gearboxes are extensively used for speed change and torque transmission in various industrial applications. It is well known that the mechanical gear has a high torque density, but suffers from some inherent problems such as contact friction, noise, and heat, while vibration and reliability are of great concern. In contrast, the magnetic gear (MG) offers significant advantages of reduced acoustic noise, minimum vibration, free from maintenance, improved reliability, inherent overload protection, and physical isolation between the input

Received 8 August 2012, Accepted 15 October 2012, Scheduled 18 October 2012

* Corresponding author: Ming Cheng (mcheng@seu.edu.cn).

and output shafts. However, for a long time, MGs have received relatively little attention, probably due to the poor torque density and relative complexity of the magnetic circuits [1, 2].

The idea of MGs can be tracked down to the beginning of the 20th century. In 1913, a US Patent Application described an electromagnetic gearing which should be the original topology [3], but almost no one was interested in it at that time. Until a MG topology quite similar to a mechanical spur gear was proposed by Faus in 1941 [4], people gradually paid attention to MGs. However, low utilization and poor performance of ferrite permanent magnet (PM) material made it impossible to be widely used in industry. Until the high-performance neodymium iron boron (NdFeB) PM material was invented in the 1980s, the research on MGs aroused great interests again. Naturally, the earlier MG topologies were converted from mechanical gear topologies. These converted MGs simply replaced the slots and teeth of iron core by N-poles and S-poles of PMs, respectively. The low utilization of PMs was the key problem which caused poor torque density.

In 2001, Atallah and Howe proposed a high-performance MG named as the coaxial magnetic gear (CMG), whose principle of operation was based on the modulation of the magnetic fields produced by two PM rotors via the ferromagnetic pole-pieces [5, 6]. Unlike the converted MGs, the CMG has a higher torque density, because all the PMs simultaneously contribute to torque transmission. Based on the field modulation principle, many improved CMG topologies are proposed to further obtain a better performance [7–12]. In view of the coaxial structure, the CMG can be artfully integrated with a high-speed outer-rotor PM brushless machine to constitute a composite electrical machine named as the magnetic-gear permanent-magnet (MGPM) machine, which can achieve low-speed high-torque driving while providing high torque density. The MGPM machine has attracted wide attention for application to wind power generation and direct-drive electric vehicles.

The purpose of this paper is to quantitatively assess those viable MGPM machines, hence identifying their key features, merits, demerits and applications. In Section 2, a comprehensive review of MGs, including the converted topologies and the field-modulated topologies, will be conducted. Then, Section 3 will be devoted to discussing three viable MGPM machines. Consequently, the performances of these MGPM machines will be quantitatively analyzed and compared in Section 4. Finally, conclusions will be drawn in Section 5.

2. REVIEW OF MAGNETIC GEARS

2.1. Converted Magnetic Gears

In 1980, a multielement MG which employed the variable reluctance principle to transmit torque was proposed [1]. However, it not only has low torque density and complexity, but also suffers from low efficiency due to the excitation loss, core loss and brush friction. In 1987, Tsurumoto and Kikuchi proposed an involute magnetic gear shown in Figure 1, which was a new transmission type at that time [2]. Later, the magnetic worm gear and skew gear have also been presented in the literature [13,14]. The complicated arrangement of magnetic worm gear is illustrated in Figure 2. In addition to complexity, all these MGs have a poor torque density, less than 2 kNm/m^3 , mainly due to the bulky package and low utilization of PMs.

Abandoning the complicated magnetic worm gear and skew gear, people once again focused on analyzing and studying the simple parallel-axis MGs which were firstly proposed by Ikuta [15]. The parallel-axis MGs include two different magnetic coupling types: radial coupling and axial coupling. Figure 3 shows two different topologies of radial coupling, while Figure 4 shows an axial coupling topology. In [16,17], the influence of parameters on the torque of an external parallel-axis MG with a velocity ratio of 1 : 1 has been detailedly investigated with the help of finite element analysis (FEA). Moreover, in [18,19], the corresponding two-dimensional analytical calculation approach has been developed and exhibits a good agreement with the FEA results. In addition, Yao et al. also studied the magnetic coupling characteristics of a perpendicular-axis MG shown in Figure 5 [20]. Although the configuration of parallel-axis or perpendicular-axis MGs is very simple, their torque density is so low that they cannot be widely used.

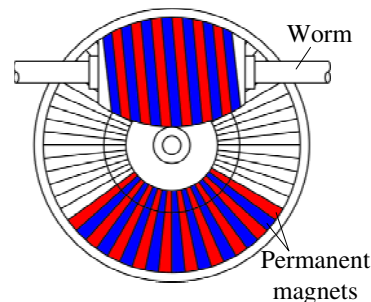
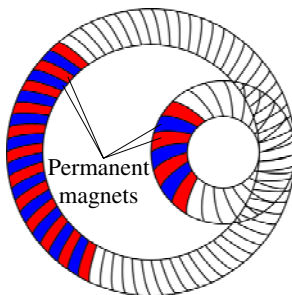


Figure 1. Involute magnetic gear. **Figure 2.** Magnetic worm gear.

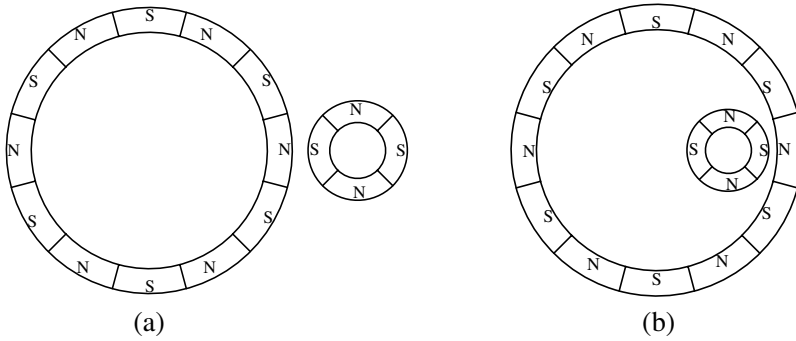


Figure 3. Radial-coupling parallel-axis MGs. (a) External type. (b) Internal type.

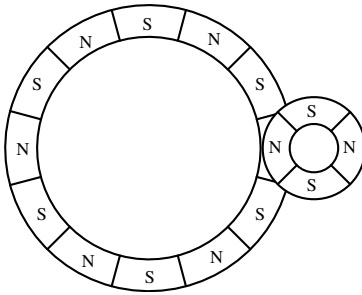


Figure 4. Axial-coupling parallel-axis MG.

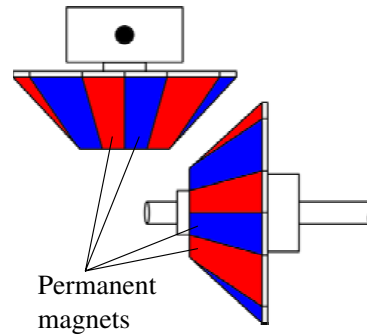


Figure 5. Perpendicular-axis MG.

A particular type of the converted MGs is the magnetic torque coupler which can be used to transmit torque between the two coupling halves at the same speed [21]. There are two types of magnetic torque couplers, namely axial and coaxial couplers as shown in Figure 6. In [22, 23], parametric analysis of axial coupler is carried out with both FEA and torque formula established by Furlani in [24]. In [25–27], the coupling performances of the coaxial coupler are presented, which is useful for product design and analysis. With the advantages of high torque transmission capability and overload protection, these couplers can be used in seal-less pumps, process and chemical industries, and other applications where the driving and driven parts need to be separated.

Referencing to the structure of the mechanical planetary gear and the operating principle of parallel-axis MGs, a magnetic planetary

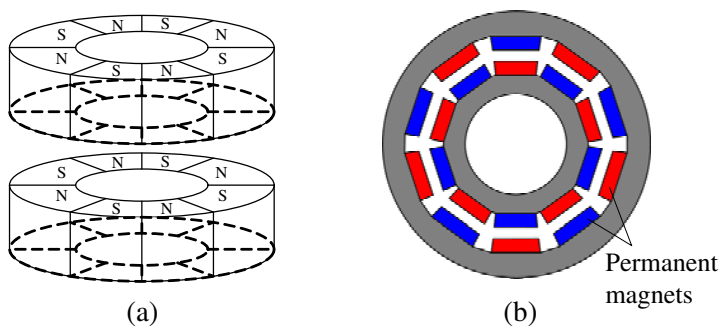


Figure 6. Magnetic torque couplers. (a) Axial coupler. (b) Coaxial coupler.

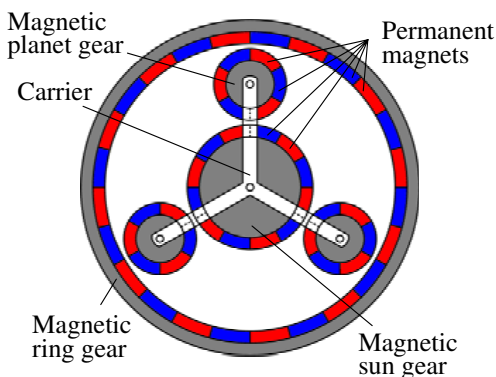


Figure 7. Magnetic planetary gear.

gear (MPG) as shown in Figure 7 has been proposed and analyzed in [28]. In addition to the advantages of the parallel-axis MGs, the MPG has the characteristics of three transmission modes, a high-speed-reduction ratio, and a high torque density. Literature [28] pointed out that the number of magnetic planet gears is the key to improve the MPG transmitted torque. By using the FEA, the MPG with six magnetic planet gears exhibits nearly 100 kNm/m^3 of shear stress on the magnetic ring gear [28]. Thus, there is an increasing interest in the MPG for various applications, such as wind power generation and electric propulsion.

Although various converted MGs have been delineated, it is important to make a comparison with the mechanical gear. Table 1 summarizes the converted MGs and compares them with a mechanical spur gear, with emphasis on the torque density. It is seen that

Table 1. Comparison of converted MGs with mechanical spur gear.

Gear type	Transmission rate	Operating principle	Torque density [kNm/m ³]	Complexity	Utilization of PMs
Mechanical spur gear	1.4–28000	Mechanical meshing	100–200	No	NA
Multielement MG [1]	24 : 1	Variable reluctance	3.96	Yes	Electrical excitation
Involute MG [2]	3 : 1	Magnetic meshing	1.7		Low
Magnetic worm gear [13]	33 : 1		0.74		
Magnetic skew gear [14]	1.7 : 1		0.15		
Parallel-axis MG [19]	4 : 1		11.6	No	
Perpendicular-axis MG [20]	1 : 1		3		
Magnetic torque coupler [26]	1 : 1		51.9		
MPG [28]	3 : 1		97.3		Low

all converted MGs (except the magnetic torque coupler and MPG) have low torque density less than 12 kNm/m³, which is far less than that provided by the mechanical spur gear. Such low torque density seriously limits their popularization and application. In addition, although the magnetic torque coupler and MPG have a high torque density, the former can not achieve variable speed driving, while the latter has a low utilization of PMs.

2.2. Field-modulated Magnetic Gears

In 2001, Atallah and Howe proposed the CMG as shown in Figure 8, which was completely different from the converted MGs. It employs PMs on the both outer and inner rotors, and has ferromagnetic pole-pieces between the two rotors. Its operation relies on the use of the ferromagnetic pole-pieces to modulate the magnetic fields produced by each of the PM rotors [5, 6, 29]. Due to the contribution of all PMs to the torque transmission, it exhibits a high torque density, namely 50–150 kNm/m³.

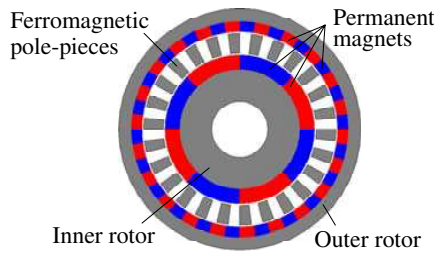


Figure 8. Coaxial magnetic gear.

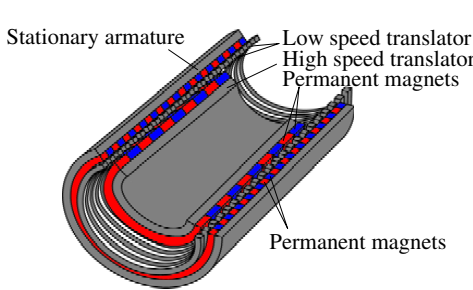


Figure 9. Linear MG.

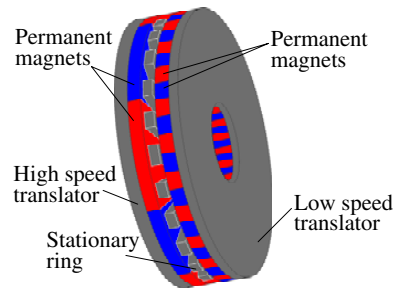


Figure 10. Axial-field MG.

Following the operating principle of CMG, Atallah et al. also proposed and analyzed other two forms of field-modulated MGs: the linear MG [30, 31] and the axial-field MG [32] as shown in Figure 9 and Figure 10, respectively. The linear MG can have a transmitted force density in excess of 1.7 MN/m^3 with NdFeB magnets. Thus, when combined with a linear PM brushless motor [33], it can offer significant advantages in many applications, such as wave power generation [34] and railway traction. Similarly, the axial-field MG is particularly suitable for applications where a hermetic isolation between input and output shafts is required, such as pumps for use in the chemical, food, and aerospace industries. It is reported that a torque density exceeding 70 kNm/m^3 can be achieved in the axial-field MG, and the axial force exerted on the high speed and low speed rotors is relatively low [32].

The CMG proposed by Atallah is installed with radially magnetized (RM) PMs mounted on the surfaces of both outer and inner rotors, hence termed the CMGRM, which is shown in Figure 11(a). Different from radially magnetized arrangement, Halbach PM arrays hold some attractive features, namely, near-sinusoidal airgap flux density distribution, strong field intensity, and good self-shielding magnetization [35, 36]. So, Jian and Chau incorporated the attractive

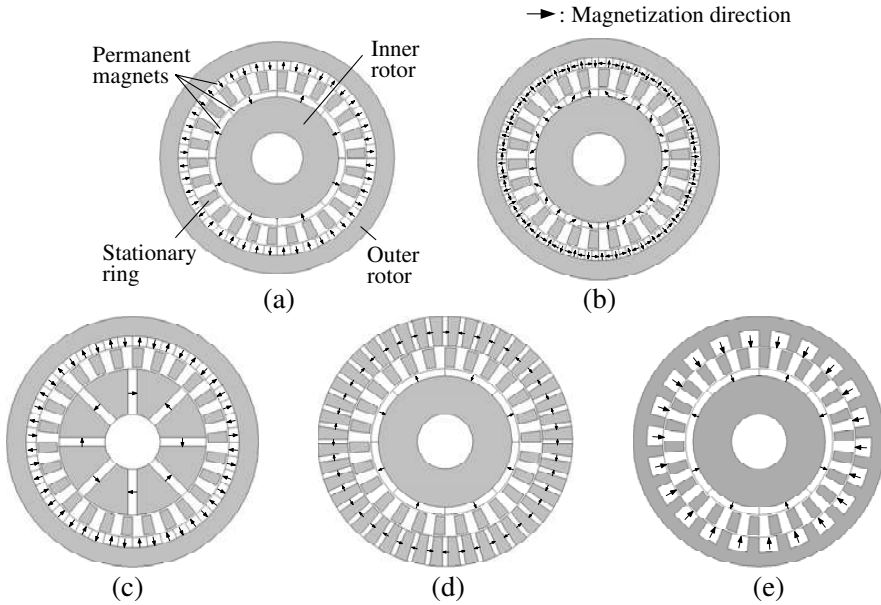


Figure 11. Different CMG topologies. (a) CMGRM. (b) CMGHM. (c) CMGTM-IR. (d) CMGTM-OR. (e) CMGSM-OR.

features of Halbach magnetized (HM) arrays into the CMG to form a topology termed the CMGHM as shown in Figure 11(b) to further improve the performance of CMG [7, 8]. However, considering the centrifugal force and mechanical stress, the surface-mounted type is not suitable for high-speed or high-torque transmission. So, Rasmussen et al. proposed a spoke type [9], namely, the interior PMs of the inner rotor (IR) are tangentially magnetized (TM), hence termed the CMGTM-IR as shown in Figure 11(c), which can offer the flux-concentrating effect and high mechanical reliability. Following the design of CMGTM-IR, the CMG with the interior PMs in the outer rotor (OR) is named as the CMGTM-OR as shown in Figure 11(d) [37]. To further improve the mechanical integrity and save PMs, in [10], Liu et al. proposed and analyzed a unique topology which inserts the same-polarity magnetized (SM) PMs into the iron core along the circumference of the outer rotor to simplify the manufacturing process while the torque density is maintained, which is referred as the CMGSM-OR as shown in Figure 11(e). In [38], the transient performance of CMGs is analyzed and discussed by employing finite element co-modeling which can provide efficient and accurate results.

Although many CMG topologies have been proposed, a

Table 2. Key parameters for CMG comparison.

Parameters	Value
Number of pole-pairs on inner rotor	4
Number of pole-pairs on outer rotor	22
Number of ferromagnetic pole-pieces	26
Outside radius of outer rotor [mm]	74
Inside radius of outer rotor [mm]	56.5
Outside radius of stationary ring [mm]	55.5
Inside radius of stationary ring [mm]	44.2
Outside radius of inner rotor [mm]	43.2
Inside radius of inner rotor [mm]	16.2
Axial length [mm]	100
Airgap length [mm]	1

quantitative comparison is absent in literature. Based on the same key parameters as listed in Table 2, the comparison results are summarized in Table 3. It can be seen that the CMGHM is most favorable when the torque density and torque ripple are of the main concern. However, the magnetization process of CMGHM is so difficult that it is hard to implement. In addition, when the transmitted torque or rotational speed is very high, the mechanical reliability becomes important which rules out the surface-mounted PM structure.

Since MGs have many advantages over mechanical gears, it is an important work to further compare the most common CMGRM [6] with various mechanical gears under similar input velocity, transmission rate and output torque. Table 4 shows the comparison results of four commercial mechanical gears with the CMGRM in terms of volume, weight, efficiency, initial cost and service life. It can be found that the CMGRM is more favorable when the volume, weight and efficiency are of main concern. In addition, due to contact-free, the service life of CMGRM is much longer than that of the mechanical gears. However, because of the high cost of PMs, the initial cost of the CMGRM is higher than that of the mechanical gears. Probably, the merit of free from maintenance of the CMGRM may compensate for the cost difference. Of course, some aspects of the CMGs still need to be improved, such as the thermal instability and accidental demagnetization of PMs as well as instability of the instantaneous transmission rate and fluctuation of the driving torque.

Table 3. Comparison of different CMG topologies.

CMG topologies	Torque density [kNm/m ³]	Torque ripple	Magnetization process	Mechanical reliability
CMGRM	69.6	0.43%	Easy	Low
CMGHM	86.3	0.22%	Difficult	
CMGTM-IR	58.3	0.79%	Easy	Medium
CMGTM-OR	81.7	1.12%		
CMGSM-OR	62.4	0.96%		High

Table 4. Comparison of CMGRM with commercial mechanical gears.

Gear topologies	Lean gear — worm gear deceleration	Lean gear deceleration	Lean gear — spiral umbrella gear deceleration	Parallel shaft lean gear deceleration	CMGRM [6]
Transmission rate	7.81	6	5.7	5.54	5.75
Input velocity [r/min]	1500				
Output velocity [r/min]	192	250	263	271	261
Output torque [Nm]	54.74	57.32	54.49	52.88	55
Size [cm ³]	3970	7410	4000	4680	769
Weight [kg]	10.1	9.8	11.2	12.9	4.6
Efficiency	75%	95%			> 97%
Initial cost [\$]	236.9	221.2	308.1	260.7	472
Service life [years]	3–5				> 10

3. VIABLE TOPOLOGIES OF MGPM MACHINES

With ever increasing demand of electric direct-drive, the design, analysis and realization of low-speed high-torque machines are more and more attractive. In recent years, many high-performance PM brushless machines such as the doubly salient machine, flux-reversal machine, flux-switching machine, and transverse-field machine have

been proposed for direct-drive systems [39-43]. However, they inevitably suffer from the problem of low torque density due to the low-speed requirement for motor design. It is noteworthy that the CMG can readily be integrated into the PM brushless machine to form the MGPM machine, in which the low-speed requirement for direct-drive and the high-speed requirement for motor design can be achieved simultaneously. This type of machine can offer significant advantages for application to wind power generation, electric vehicles, and electric ship propulsion [44, 45].

Naturally, an outer-rotor PM brushless machine can be combined with any kind of CMGs mentioned above to form a MGPM machine. According to the number of air gaps, the existing MGPM machines can be classified as three viable topologies as shown in Figure 12. Relatively speaking, the concept of the three-airgap MGPM machine (Figure 12(a)) is so straightforward that it was proposed first, and its characteristics have been extensively studied [46, 47]. In essence, the three-airgap topology is a simple combination of an outer-rotor PM machine with a CMG, in which the interaction of magnetic field distributions between the embedded PM machine and the outer gear is insignificant. The reported results show that the three-airgap MGPM machine can offer a high torque density when employing a CMG with a gear ratio between 5 : 1 and 10 : 1, while a high power factor of the

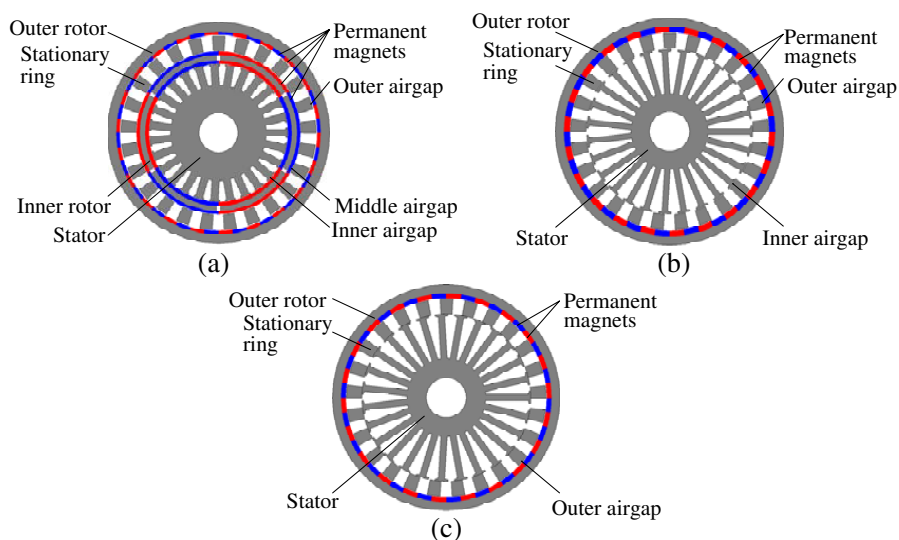


Figure 12. Viable MGPM machines. (a) Three-airgap topology. (b) Two-airgap topology. (c) One-airgap topology.

outer-rotor PM machine can be maintained [6]. However, this kind of machine has two rotating parts and three airgaps, whose mechanical construction is so complicated that it is difficult to manufacture.

As already mentioned in the CMGs, due to the introduction of the stationary ring, the magnetic field produced by PMs on the gear outer rotor can be modulated into a series of space harmonics. By using the highest asynchronous high-speed rotary space harmonic to transmit torque, a two-airgap MGPM machine shown in Figure 12(b) has been proposed [48, 49], which has a simpler configuration than the three-airgap topology. Moreover, due to the relative stillness of the stationary ring and the stator, the airgap between them can be removed. So, the so-called one-airgap topology is deduced as shown in Figure 12(c). When the number of ferromagnetic pole-pieces is integer multiple of the number of stator teeth, a particular one-airgap MGPM machine can be obtained and has been analyzed [50, 51], which is actually similar to the PM vernier machine [52, 53]. Compared with the three-airgap topology, the operation of the two-airgap and one-airgap topologies relies on the flux modulation, namely the number of pole-pairs of stator armature winding should be equal to the number of pole-pairs of the modulated harmonic rather than the PM pole-pairs on the outer rotor.

4. PERFORMANCE COMPARISON OF MGPM MACHINES

Although the operating principle, modeling, and electromagnetic field analysis of the three types of MGPM machines have been presented, a quantitative comparison among them is absent in literature. Based on the reported modeling and mathematical analysis, the performance comparison between these three MGPM machines can provide an important foundation for their application to direct-driving systems.

For a fair comparison, the overall outside diameter, axial length and airgap length of the three MGPM machines are the same, which are actually the dimensions of the three-airgap MGPM machine designed in [46]. Meanwhile, the results presented in this section are based on the optimal design of individual MGPM machines by using the FEA. The corresponding design data and results are summarized in Table 5. Figure 13 and Figure 14 show the no-load magnetic field distributions and the corresponding radial flux density waveforms at the location of stator outside diameter, respectively. The stator winding connection is shown in Figure 15. It can be seen that the 3-phase symmetric windings consist of 27 double-layer coils. Each coil span covers 4 slot pitches, and the pole pitch is $9/2$ of the slot pitch. Hence, the no-

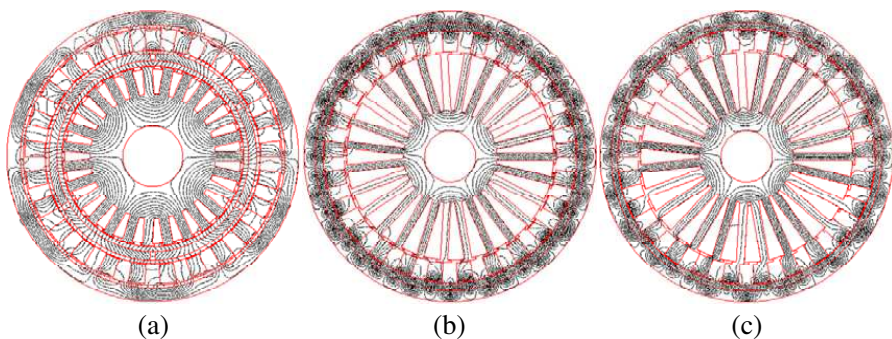


Figure 13. No-load magnetic field distributions. (a) Three-airgap topology. (b) Two-airgap topology. (c) One-airgap topology.

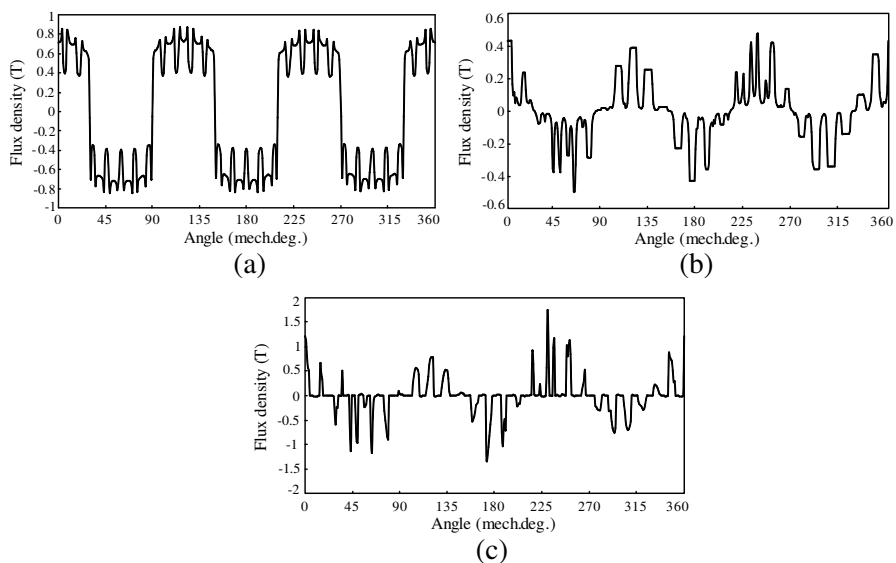


Figure 14. No-load radial flux density waveforms at stator outside diameter. (a) Three-airgap topology. (b) Two-airgap topology. (c) One-airgap topology.

load EMF waveforms at the rated speed can be deduced as shown in Figure 16. Consequently, the cogging torque and full-load outer-rotor output torque waveforms are simulated as shown in Figures 17 and 18, respectively.

From Table 5, it can be found that the one-airgap MGPM machine provides the largest rated power for the same machine size. Although

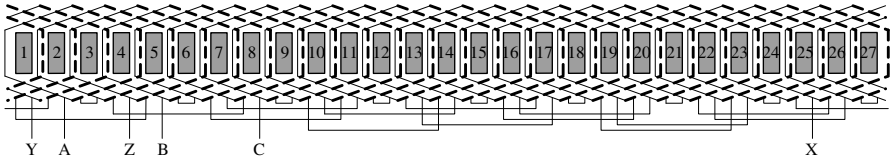


Figure 15. Stator winding connection diagram of three MGPM machines.

Table 5. Key design data and results of MGPM machines.

MGPM machine type	Three-airgap	Two-airgap	One-airgap
Rated power [W]	3000	2500	3200
Rated phase voltage [V]	36		
Rated outer-rotor speed [rpm]	600		
No. of phases	3		
No. of outer-rotor pole-pairs	22		
No. of ferromagnetic pole-pieces	25		
No. of stator pole-pairs	3		
No. of stator slots	27		
No. of turns per phase winding	27	90	72
Winding package factor	46%		
Rated current density [A/mm^2]	5		
Overall outside diameter [mm]	194		
Inside radius of stator [mm]	17		
Thickness of stationary ring [mm]	13		
Inner airgap length [mm]	0.6	0.6	
Middle airgap length [mm]	0.6		
Outer airgap length [mm]	1	0.6	0.6
Axial length [mm]	40		
PM material	38SH		NdFeB
Total copper volume [cm^3]	96.7	278.9	265.4
Total PM volume [cm^3]	132.5	109.3	88
Torque per mass [Nm/kg]	6.36	5.03	6.43
Torque per PM volume [kNm/m^3]	360.8	364.1	578.4

the three-airgap topology also produces a larger power output than the two-airgap one, it has a more complicated construction. It should be noted that the three-airgap topology desires much more PM materials

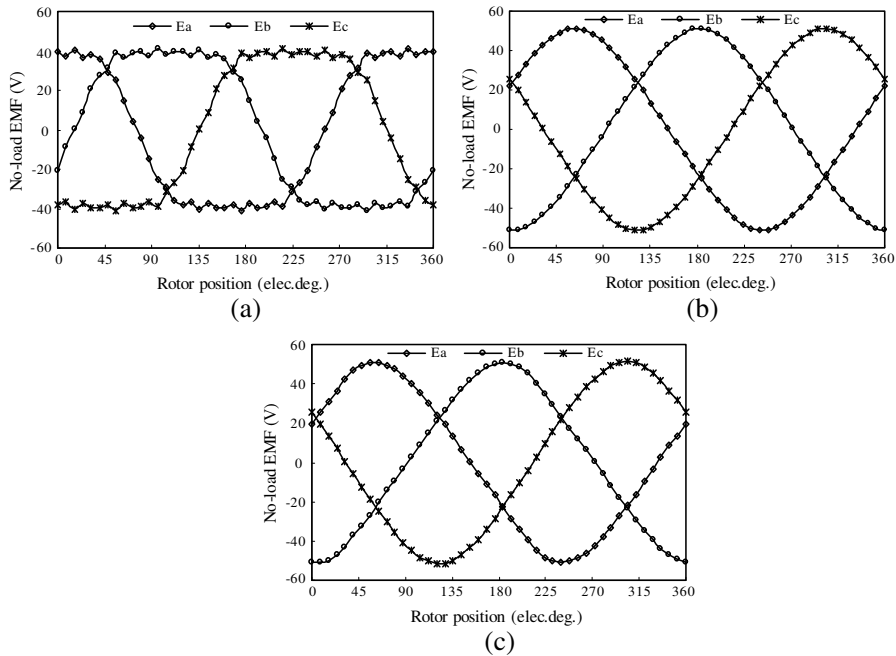


Figure 16. No-load EMF waveforms. (a) Three-airgap topology. (b) Two-airgap topology. (c) One-airgap topology.

because it needs to mount three layers of PMs on two rotors, which undoubtedly increases the manufacturing cost. Meanwhile, due to removing one airgap, the total PM volume of the one-airgap topology is about one fifth less than that consumed in the two-airgap topology. Concerning the torque per mass, the three-airgap topology is almost the same as the one-airgap topology, which is over 25% larger than the two-airgap topology. However, from the view of the torque per PM volume, one-airgap topology is absolutely dominant, especially facing the high cost of PM materials at present.

Due to the dependence of harmonic magnetic field for operation, the no-load stator-tooth flux density of the two-airgap and one-airgap topologies is very low as indicated in Figure 14, resulting in a much more winding turns for the same rated phase voltage compared to the three-airgap topology at the same operating frequency. So a deep-slot structure must be adopted in these two types of machines in order to obtain an optimal power output, which inevitably increases the total copper consumption.

From Figure 16, it can be seen that although adopting the same

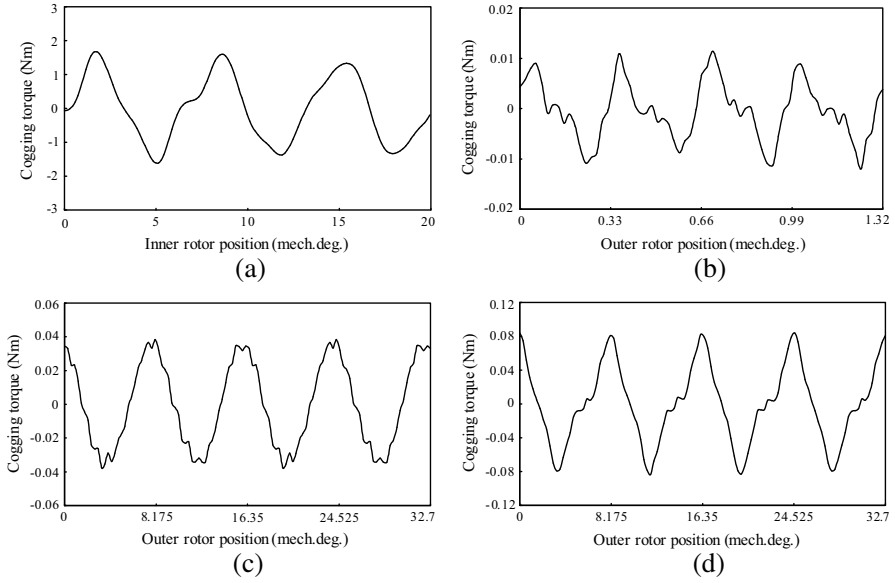


Figure 17. Cogging torque waveforms. (a) Inner rotor of three-airgap topology. (b) Outer rotor of three-airgap topology. (c) Outer rotor of two-airgap topology. (d) Outer rotor of one-airgap topology.

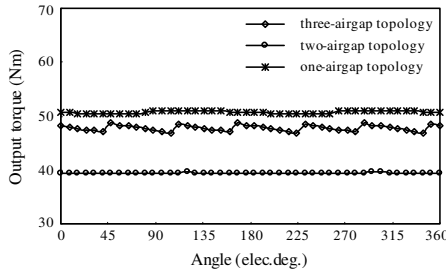


Figure 18. Outer-rotor output torque waveforms at full-load operation.

distributed winding connection as shown in Figure 15, the no-load EMF of the three-airgap topology generated by the inner-airgap 180° square-wave magnetic field as shown in Figure 14(a) is nearly a 120° square waveform, while the no-load EMF of the two-airgap and one-airgap topologies produced by the modulated harmonic sinusoidal magnetic field are quasi-sinusoidal waveforms. Therefore, the brushless DC control is more suitable for the three-airgap topology, and the brushless AC control is preferable for the two-airgap and one-airgap topologies.

From Figure 17, it can be observed that the cogging torque in the outer rotor of three different MGPM machines is very low. However, the magnitude of the cogging torque in the inner rotor of the three-airgap topology is about 1.7 Nm which is relatively large and could affect the machine performance. This inner-rotor cogging torque is mainly caused by the unilateral magnetic force resulted from the odd number of the stator teeth. In addition, some important findings can be observed: namely, the period of the cogging torque in the inner rotor or outer rotor of the three-airgap topology is still determined by the least common multiple of the stator teeth and rotor pole number. However, the cogging-torque period in the two-airgap and one-airgap topologies is related to the least common multiple of the rotor pole number and the greatest common divisor of the ferromagnetic pole-pieces and the number of stator teeth.

Obviously, the comparison between the one-airgap and two-airgap topologies indicates that due to the improved flux density amplitude in the stator teeth resulted from removing one airgap, the torque density of the one-airgap topology is over 25% higher than that of the two-airgap topology. However, the use of only one airgap results in higher local magnetic saturation in the stator and stronger interaction between the armature field and higher-order modulated harmonics, which increases the output torque ripple as shown in Figure 18. Meanwhile, it can be observed that the output torque in the three-airgap topology has a large fluctuation, which is mainly due to adopting 120° square-wave current control. Generally, in order to achieve stable torque output, complex control algorithms such as the harmonic current injection need to be employed.

5. CONCLUSION

In this paper, the development of MGs and hence the MGPM machines have been reviewed and discussed, with emphasis on providing performance analysis and hence a quantitative comparison of three viable MGPM machines. Between the two major families of MGs, the field-modulated CMGs are preferred to the converted MGs due to their better utilization of PM material and hence higher torque density as well as their capability of integration into the PM brushless machines to form the MGPM machines. Among the three major topologies of MGPM machines, the one-airgap topology is most suitable for low-speed high-torque direct-drive applications because of its highest torque density, minimum use of PM material and simplest structure. Nevertheless, the three-airgap topology has the potentiality to make use of two rotors to perform electric variable transmission for hybrid vehicles.

ACKNOWLEDGMENT

This work was supported in part by a grant (Project 51177013) from the National Natural Science Foundation of China, a grant (Project BK2010013) from Innovative Scholar Ascent Program of Jiangsu Province, China, and a grant (Project: 2013CB035603) from the 973 Program of China.

REFERENCES

1. Hesmondhalgh, D. E. and D. Tipping, "A multielement magnetic gear," *IEE Proceedings*, Vol. 127, No. 3, 129–138, 1980.
2. Tsurumoto, K. and S. Kikuchi, "A new magnetic gear using permanent magnet," *IEEE Transactions on Magnetics*, Vol. 23, No. 5, 3622–3624, 1987.
3. Neuland, A. H., "Apparatus for transmitting power," U.S. Patent 1 171 351, 1916.
4. Faus, H. T., "Magnet gearing," U.S. Patent 2 243 555, 1941.
5. Atallah, K. and D. Howe, "A novel high-performance magnetic gear," *IEEE Transactions on Magnetics*, Vol. 37, No. 4, 2844–2846, 2001.
6. Atallah, K., S. D. Calverley, and D. Howe, "Design, analysis and realization of a high-performance magnetic gear," *IEE Proc. — Electr. Power Appl.*, Vol. 151, No. 2, 135–143, 2004.
7. Jian, L., K. T. Chau, Y. Gong, J. Z. Jiang, C. Yu, and W. Li, "Comparison of coaxial magnetic gears with different topologies," *IEEE Transactions on Magnetics*, Vol. 45, No. 10, 4526–4529, 2009.
8. Jian, L. and K. T. Chau, "A coaxial magnetic gear with Halbach permanent-magnet arrays," *IEEE Transactions on Energy Conversion*, Vol. 25, No. 2, 319–328, 2010.
9. Rasmussen, P. O., T. O. Andersen, F. T. Jorgensen, and O. Nielsen, "Development of a high-performance magnetic gear," *IEEE Transactions on Industry Applications*, Vol. 41, No. 3, 764–770, 2005.
10. Liu, X., K. T. Chau, J. Z. Jiang, and C. Yu, "Design and analysis of interior-magnet outer-rotor concentric magnetic gears," *Journal of Applied Physics*, Vol. 105, 07F101-1–3, 2009.
11. Jian, L., G. Xu, J. Song, H. Xue, D. Zhao, and J. Liang, "Optimum design for improving modulating-effect of coaxial magnetic gear using response surface methodology and genetic

- algorithm,” *Progress In Electromagnetics Research*, Vol. 116, 297–312, 2011.
12. Ge, Y.-J., C.-Y. Nie, and Q. Xin, “A three dimensional analytical calculation of the air-gap magnetic field and torque of coaxial magnetic gears,” *Progress In Electromagnetics Research*, Vol. 131, 391–407, 2012.
 13. Kikuchi, S. and K. Tsurumoto, “Design and characteristics of a new magnetic worm gear using permanent magnet,” *IEEE Transactions on Magnetics*, Vol. 29, No. 6, 2923–2925, 1993.
 14. Kikuchi, S. and K. Tsurumoto, “Trial construction of a new magnetic skew gear using permanent magnet,” *IEEE Transactions on Magnetics*, Vol. 30, No. 6, 4767–4769, 1994.
 15. Ikuta, K., S. Makita, and S. Arimoto, “Non-contact magnetic gear for micro transmission mechanism,” *Proc. IEEE Conf. on Micro Electro Mechanical Systems*, 125–130, Nara, Japan, 1991.
 16. Yao, Y. D., D. R. Huang, C. M. Lee, S. J. Wang, D. Y. Chiang, and T. F. Ying, “Magnetic coupling studies between radial magnetic gears,” *IEEE Transactions on Magnetics*, Vol. 33, No. 5, 4236–4238, 1997.
 17. Yao, Y. D., D. R. Huang, C. C. Hsieh, D. Y. Chiang, and S. J. Wang, “Simulation study of the magnetic coupling between radial magnetic gears,” *IEEE Transactions on Magnetics*, Vol. 33, No. 2, 2203–2206, 1997.
 18. Furlani, E. P., “A two-dimensional analysis for the coupling of magnetic gears,” *IEEE Transactions on Magnetics*, Vol. 33, No. 3, 2317–2321, 1997.
 19. Jorgensen, F. T., T. O. Andersen, and P. O. Rasmussen, “Two dimensional model of a permanent magnet spur gear,” *Industry Applications Conference*, 261–265, 2005.
 20. Yao, Y. D., D. R. Huang, C. C. Hsieh, D. Y. Chiang, S. J. Wang, and T. F. Ying, “The radial magnetic coupling studies of perpendicular magnetic gears,” *IEEE Transactions on Magnetics*, Vol. 32, No. 5, 5061–5063, 1996.
 21. Yonnet, J. P., “A new type of permanent magnet coupling,” *IEEE Transactions on Magnetics*, Vol. 17, No. 6, 2991–2993, 1981.
 22. Wang, R., E. P. Furlani, and Z. J. Cendes, “Design and analysis of a permanent magnet axial coupling using 3D finite element field computations,” *IEEE Transactions on Magnetics*, Vol. 30, No. 4, 2292–2295, 1994.
 23. Yao, Y. D., G. J. Chiou, D. R. Huang, and S. J. Wang, “Theoretical computations for the torque of magnetic coupling,”

- IEEE Transactions on Magnetics*, Vol. 31, No. 3, 1881–1884, 1995.
24. Furlani, E. P., “Formulas for the force and torque of axial couplings,” *IEEE Transactions on Magnetics*, Vol. 29, No. 5, 2295–2301, 1993.
 25. Hornreich, R. M. and S. Shtrikman, “Optimal design of synchronous torque couplers,” *IEEE Transactions on Magnetics*, Vol. 14, No. 5, 800–802, 1978.
 26. Wu, W., H. C. Lovatt, and J. B. Dunlop, “Analysis and design optimization of magnetic couplings using 3D finite element modeling,” *IEEE Transactions on Magnetics*, Vol. 33, No. 5, 4083–4085, 1997.
 27. Elies, P. and G. Lemarquand, “Analytical study of radial stability of permanent-magnet synchronous couplings,” *IEEE Transactions on Magnetics*, Vol. 35, No. 4, 2133–2136, 1999.
 28. Huang, C. C., M. C. Tsai, D. G. Dorrell, and B. J. Lin, “Development of a magnetic planetary gearbox,” *IEEE Transactions on Magnetics*, Vol. 44, No. 3, 403–412, 2008.
 29. Jian, L. and K. T. Chau, “Analytical calculation of magnetic field distribution in coaxial magnetic gears,” *Progress In Electromagnetics Research*, Vol. 92, 1–16, 2009.
 30. Atallah, K., J. Wang, and D. Howe, “A high-performance linear magnetic gear,” *Journal of Applied Physics*, Vol. 97, 10N516-1–3, 2005.
 31. Li, W. and K. T. Chau, “Analytical field calculation for linear tubular magnetic gears using equivalent anisotropic magnetic permeability,” *Progress In Electromagnetics Research*, Vol. 127, 155–171, 2012.
 32. Mezani, S., K. Atallah, and D. Howe, “A high-performance axial-field magnetic gear,” *Journal of Applied Physics*, Vol. 99, 08R303-1–3, 2006.
 33. Chau, K. T., W. Li, and C. H. T. Lee, “Challenges and opportunities of electric machines for renewable energy,” *Progress In Electromagnetics Research B*, Vol. 42, 45–74, 2012.
 34. Li, W., K. T. Chau, and J. Z. Jiang, “Application of linear magnetic gears for pseudo-direct-drive oceanic wave energy harvesting,” *IEEE Transactions on Magnetics*, Vol. 47, No. 10, 2624–2627, 2011.
 35. Halbach, K., “Design of permanent multipole magnets with oriented rare earth cobalt material,” *Nuclear Instruments and Methods*, Vol. 169, 1–10, 1980.
 36. Choi, J.-S. and J. Yoo, “Design of a Halbach magnet array based

- on optimization techniques," *IEEE Transactions on Magnetics*, Vol. 44, No. 10, 2361–2366, 2008.
37. Li, X., K. T. Chau, M. Cheng, W. Hua, and Y. Du, "An improved coaxial magnetic gear using flux focusing," *International Conference on Electrical Machines and Systems*, 1–4, Beijing, China, 2011.
 38. Chau, K. T., D. Zhang, J. Z. Jiang, and L. Jian, "Transient analysis of coaxial magnetic gears using finite element co-modeling," *Journal of Applied Physics*, Vol. 103, 07F101-1–3, 2008.
 39. Liao, Y. F., F. Liang, and T. A. Lipo, "A novel permanent magnet motor with doubly salient structure," *IEEE Transactions on Industry Applications*, Vol. 31, No. 5, 1069–1078, 1995.
 40. Zhu, Z. Q., Y. Pang, D. Howe, S. Iwasaki, R. Deodhar, and A. Pride, "Analysis of electromagnetic performance of flux-switching permanent-magnet machines by nonlinear adaptive lumped parameter magnetic circuit model," *IEEE Transactions on Magnetics*, Vol. 41, No. 11, 4277–4287, 2005.
 41. Cheng, M., W. Hua, J. Zhang, and W. Zhao, "Overview of stator-permanent magnet brushless machines," *IEEE Transactions on Industrial Electronics*, Vol. 58, No. 11, 5087–5101, 2011.
 42. Touati, S., R. Ibtouen, O. Touhami, and A. Djerdir, "Experimental investigation and optimization of permanent magnet motor based on coupling boundary element method with permeances Network," *Progress In Electromagnetics Research*, Vol. 111, 71–90, 2011.
 43. Zhao, W., M. Cheng, R. Cao, and J. Ji, "Experimental comparison of remedial single-channel operations for redundant flux-switching permanent-magnet motor drive," *Progress In Electromagnetics Research*, Vol. 123, 189–204, 2012.
 44. Jian, L., G. Xu, Y. Gong, J. Song, J. Liang, and M. Chang, "Electromagnetic design and analysis of a novel magnetic-gear-integrated wind power generator using time-stepping finite element method," *Progress In Electromagnetics Research*, Vol. 113, 351–367, 2011.
 45. Jian, L. and K.-T. Chau, "Design and analysis of a magnetic-gear electronic-continuously variable transmission system using finite element method," *Progress In Electromagnetics Research*, Vol. 107, 47–61, 2010.
 46. Chau, K. T., D. Zhang, J. Z. Jiang, C. Liu, and Y. Zhang, "Design of a magnetic-gear outer-rotor permanent magnet brushless motor for electric vehicles," *IEEE Transactions on Magnetics*,

- Vol. 43, No. 6, 2504–2506, 2007.
47. Jian, L., K. T. Chau, and J. Z. Jiang, “A magnetic-gearred outer-rotor permanent-magnet brushless machine for wind power generation,” *IEEE Transactions on Industry Applications*, Vol. 45, No. 3, 954–962, 2009.
 48. Wang, L. L., J. X. Shen, P. C. K. Luk, W. Z. Fei, C. F. Wang, and H. Hao, “Development of a magnetic-gearred permanent magnet brushless motor,” *IEEE Transactions on Magnetics*, Vol. 45, No. 10, 4578–4581, 2009.
 49. Fan, Y., H. Jiang, M. Cheng, and Y. Wang, “An improved magnetic-gearred permanent magnet in-wheel motor for electric vehicles,” *IEEE Vehicle Power and Propulsion Conference*, Lille, France, 2010.
 50. Toba, A. and T. A. Lipo, “Generic torque-maximizing design methodology of surface permanent-magnet vernier machine,” *IEEE Transactions on Industry Applications*, Vol. 36, No. 6, 1539–1546, 2000.
 51. Li, J., K. T. Chau, J. Z. Jiang, C. Liu, and W. Li, “A new efficient permanent-magnet vernier machine for wind power generation,” *IEEE Transactions on Magnetics*, Vol. 46, No. 6, 1475–1478, 2010.
 52. Liu, C. and K.-T. Chau, “Electromagnetic design and analysis of double-rotor flux-modulated permanent-magnet machines,” *Progress In Electromagnetics Research*, Vol. 131, 81–97, 2012.
 53. Xu, G., L. Jian, W. Gong, and W. Zhao, “Quantitative comparison of flux-modulated interior permanent magnet machines with distributed windings and concentrated windings,” *Progress In Electromagnetics Research*, Vol. 129, 109–123, 2012.